PHYSICAL REVIEW B **91**, 180302(R) (2015)

Effect of long- and short-range order on SiGe alloy thermal conductivity: Molecular dynamics simulation

Christopher H. Baker* and Pamela M. Norris†
Department of Mechanical and Aerospace Engineering, University of Virginia, 122 Engineer's Way, Charlottesville, Virginia 22904-4746, USA
(Received 6 March 2015; published 12 May 2015)

We report the role of long- and short-range order on the thermal conductivity and mode relaxation times of a model $Si_{0.5}Ge_{0.5}$ alloy using molecular dynamics simulation. All interactions used the Stillinger-Weber potential and the Si and Ge atoms differed only by their mass. The simulated alloys were generated using a Monte Carlo approach to decouple the short-range order from the long-range order. The thermal conductivity is almost entirely determined by the alloy's nearest-neighbor short-range order. Changes to the mode relaxation times between ∼3 and ∼6 THz upon short-range ordering, and the observed f^{-2} power law trend, suggest that short-range ordering reduces the anharmonic scattering rate of low frequency modes. The trend of thermal conductivity with short-range order may be transferred to real $Si_{0.5}Ge_{0.5}$ and other semiconductor alloys to the extent that scattering from mass disorder dominates their thermal conductivities.

DOI: 10.1103/PhysRevB.91.180302 PACS number(s): 66.70.Df, 63.50.Gh, 61.66.Dk, 61.43.Bn

Altering the composition of $Si_{1-x}Ge_x$ and other alloys is one route for engineering their thermal conductivity k [1,2]. In addition to numerous experimental studies [3–6], there have been many recent computational studies of the thermal properties of SiGe using classical molecular dynamics [7–12] and density functional theory [13,14]. Studies have focused on the dependence of k on composition [7,14], grain size [10], nanoparticle inclusions [13,15], and nanowire boundary scattering [16], all in an effort to improve the thermoelectric figure of merit [17,18]. Alloys possess two additional degrees of freedom for tuning k: the arrangement of the atoms on the lattice as characterized by the long-range [19] and short-range [20] order parameters. In molecular dynamics studies of a Lennard-Jones alloy, Duda *et al.* showed that the long-range order can be used to tune k over an order of magnitude at low temperatures [21,22]. Here, we take $Si_{0.5}Ge_{0.5}$ as a representative model for semiconductor alloys and we report the effect of long-range and short-range order on the thermal conductivity and normal mode relaxation times at 300 K using molecular dynamics simulation.

The Bragg-Williams long-range order parameter $\mathbb{L}$ gives the probability that an atom occupies the correct lattice site with reference to the ordered structure, and the probability is duly normalized by the atom's concentration in the alloy [19]. The Warren-Cowley short-range order parameters give the probability of an atom having the correct neighbor in a certain neighbor shell with reference to the ordered structure [20]. We define a set of short-range order parameters $\mathbb{S}_i$, where i indexes the neighbor shells, as the square root of the Warren-Cowley short-range order parameters so that $\lim_{i\to\infty} \mathbb{S}_i = \mathbb{L}$ [20,23]. Assuming an equimolar binary alloy for which each lattice site is eligible for a disordering substitution simplifies the expressions for $\mathbb{L}$ and $\mathbb{S}_i$. Then, $\mathbb{L} \equiv |R - W|/N$, where R (W) is the number of atoms occupying the right (wrong) lattice site, and N is the total number of atoms [23]. Similarly, $\mathbb{S}_i \equiv \sqrt{|R_i - W_i|/N_i}$, where R_i, W_i, and N_i are the numbers of right, wrong, and total neighbor pairs in neighbor shell i, respectively [23].

Structures with varying $\mathbb{L}$ and $\mathbb{S}_1$ can be generated by a Monte Carlo approach. For a binary alloy with the aforementioned simplifying assumptions, the seed structure is formed from the definition of $\mathbb{L}$ and the compositional constraint. Beginning from a zincblende reference structure [24], we randomly selected and exchanged n Si atoms and n Ge atoms, where $n = N(1 - \mathbb{L})/4$. At this point, $\mathbb{S}_i \approx \mathbb{L}$. Then, in each Monte Carlo step, we randomly selected atoms to swap that preserved the composition and $\mathbb{L}$, accepting swaps that brought $\mathbb{S}_1$ closer to the target value. No consideration has been given to the temperature or configurational entropy of these structures—they are not in equilibrium. Control over $\mathbb{L}$ and $\mathbb{S}_i$ in actual $Si_{0.5}Ge_{0.5}$ requires a nonequilibrium growth process [25,26], which is likely the case for other semiconductor alloys, too.

We used the Green-Kubo method [27,28] at thermal equilibrium to measure k. The convergence time of the heat current autocorrelation function was determined by the *first avalanche* criterion [29] with an averaging window of 8.0 ps (8^3 and 12^3 conventional cell samples) or 40.0 ps (18^3, 28^3, or 42^3 conventional cell samples) and a noise-to-signal cutoff of 1000 [30].

The relaxation times $\tau(\nu)$ were calculated using the normal mode decomposition method [28] in the frequency domain [31]. The atomic trajectories are projected onto the harmonic normal modes (calculated using GULP [32]), then Fourier transformed and fit to a Lorentzian:

$$C\frac{\Gamma(\nu)/\pi}{[f - f_0(\nu)]^2 + \Gamma^2(\nu)} = t_f^{-1}|\dot{Q}(\nu, f)|^2. \quad (1)$$

The fit yields $\tau = 1/(4\pi\Gamma)$ and the anharmonic linear frequency f_0 for each normal mode ν. At thermal equilibrium, the coefficient C is guaranteed to be $\frac{1}{2}k_BT$ from the equipartition principle. The duration of data collection t_f ought to be much greater than the maximum $\tau(\nu)$ for the material [33]. $\dot{Q}$ is the Fourier transform of the normal mode velocity coordinate

*chb2fd@virginia.edu
†pamela@virginia.edu

$\dot{q}$ [34]: $\dot{Q} = \int_0^{t_f} \dot{q} \exp(-2\pi i f t) dt$ [35]. Due to the sharpness of the peak in $|\dot{Q}|^2$, we increased the weighting near the base by taking the decimal logarithm of each side of Eq. (1). Only points above 0.104 meV/THz (1 amu Å^{2}ps^{-1}) were used in the fit. Because the global minimum of the root mean square of the residuals lay in a narrow well surrounded by local maxima, we found it necessary to do a grid search before regression, with 31 points linearly spaced between ±0.1 THz of the peak frequency and 31 points logarithmically spaced between Γ of 10^{-5} and 10^{-1} ps^{-1}.

All simulations were performed using LAMMPS [36] with a time step of 0.5 fs. The zincblende lattice constant was set to 5.43 Å, and the Si and Ge atoms only differed in their masses: 28.09 and 72.64 amu, respectively. The Stillinger-Weber potential [37] was used for all interactions since the effect of strain on k is small compared to that of mass disorder [7]. The system was equilibrated at 300 K for 1 ns in a canonical ensemble enforced by a Nosé-Hoover thermostat [38,39] with a coupling time of 2 ps. The system was then run for an additional 1 ns in a microcanonical ensemble before data were collected for 36×2^{17} time steps (2.36 ns), printing the conduction term of the heat current every ten time steps for calculating k [40], and printing atomic velocities every 36 time steps for calculating $\tau(\nu)$.

Ten independent samples of size 8^3 conventional cells were generated for each combination of $\mathbb{L}$ and $\mathbb{S}_1$ in the range 0.0–0.9 for $\mathbb{S}_1 \geqslant \mathbb{L}$ and their thermal conductivities were calculated. The uncertainty in k is reported as twice the standard deviation of the ten calculated values. The relaxation times of 2000 normal modes were calculated for one sample of each set. These normal modes include all those below 3 THz (excluding the zero frequency modes) with the rest randomly distributed among the remaining modes. Size effects were explored for select pairs of $\mathbb{L}$ and $\mathbb{S}_1$ by increasing the domain size to 12^3, 18^3, 28^3, and 42^3 conventional cells and performing a linear extrapolation procedure [12,41,42].

While only $\mathbb{S}_1$ was used as a metric for the Monte Carlo generation, $\mathbb{S}(r)$, where r is the neighbor distance, systematically decreases towards $\mathbb{L}$ (Fig. 1). One might characterize the approach of $\mathbb{S}(r)$ toward $\mathbb{L}$ by a decay length scale, which would be less than 1.5 nm for each structure plotted in Fig. 1. The case $\mathbb{S}_1 > \mathbb{L}$ can be thought of as corresponding to an alloy composed of grains defined by antiphase boundaries. Then, $\mathbb{S}(r)$ would scale with the mean grain size and $\mathbb{L}$ would scale with the ratio of volumes occupied by phase and antiphase grains. For structures with $\mathbb{L} = 0$, $\mathbb{S}(r)$ is substantially above zero at all neighbor distances (Fig. 1). This is a consequence of the small domain size and our choice to define $\mathbb{S}_i$ using the square root. The square root amplifies the small deviations of $|R_i - W_i|/N_i$ from zero; the deviations of this ratio from the ideal value (defined with respect to $\mathbb{L}$) were about the same for all structures. The small domain size also inhibits the exact convergence of $\mathbb{S}(r)$ to $\mathbb{L}$ when $\mathbb{S}_1 \gg \mathbb{L}$. Nevertheless, the structures exhibit unique $\mathbb{S}(r)$ profiles.

To within the uncertainty, the thermal conductivity depends only on a structure's $\mathbb{S}_1$, or possibly $\mathbb{S}_i$ for small i (Fig. 2). Thus, $\mathbb{L}$ affects k to the extent that it sets the lower limit for $\mathbb{S}(r)$. Consistent with the low temperature trend observed by Duda *et al.* [22], $\partial k/\partial \mathbb{S}_1$ increases as $\mathbb{S}_1$ approaches one. We observe the same trend in k with respect to ordering because

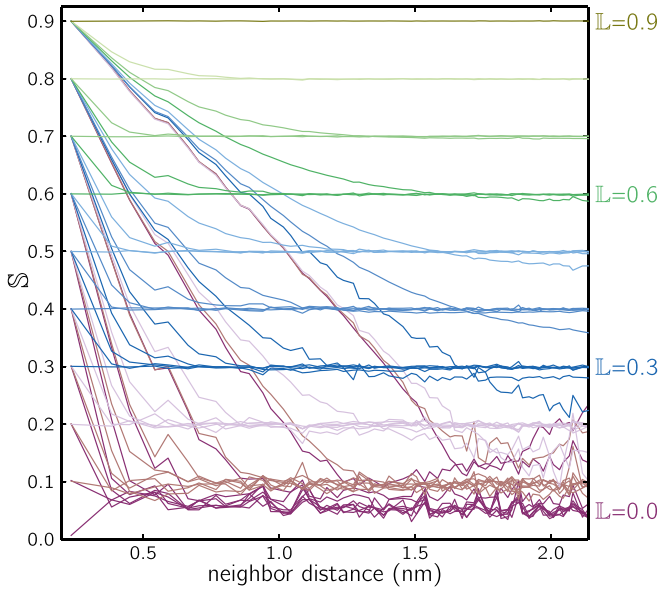

FIG. 1. (Color online) Short-range order parameters of the 8^3 unit cell SiGe structures. Each color represents a different long-range order and each line is the average of ten independently generated samples.

the structures investigated by Duda *et al.* [22], which were generated from the definition of $\mathbb{L}$, always had $\mathbb{S}_i \approx \mathbb{L}$.

A phonon is insensitive to material heterogeneities with length scales much less than the phonon's wavelength. Instead, these phonons can be thought of as traveling through a material with effective, averaged properties, e.g., density and elastic moduli [2]. *Ab initio* calculations have shown that phonons

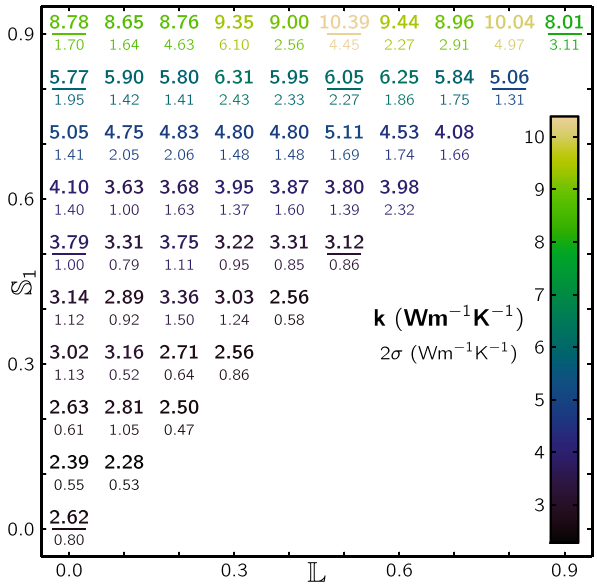

FIG. 2. (Color online) Thermal conductivities of the 8^3 unit cell SiGe structures. The thermal conductivity is constant within the uncertainty (2σ) along the rows, indicating that the short-range order is the dominant factor. Underlined data were also studied for size effects (Fig. 3).

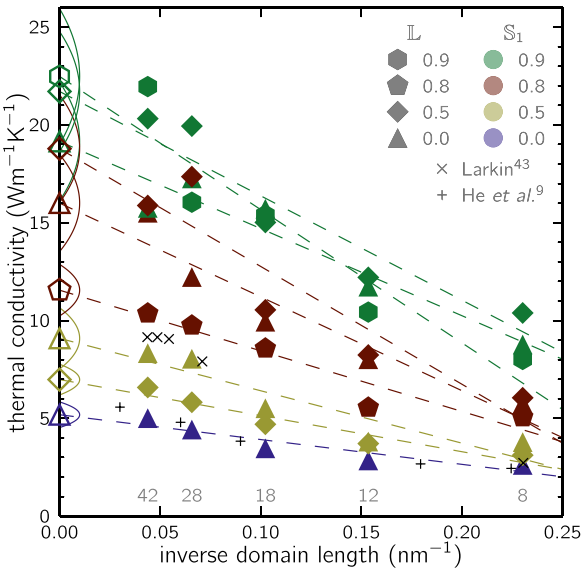

FIG. 3. (Color online) Size effects on the thermal conductivity for select SiGe structures. Each solid symbol is the average of ten samples. The arcs along the k axis indicate the 95% confidence interval of the intercept based on the 50 total samples for each ($\mathbb{L}$,$\mathbb{S}_1$) pair. The intercepts are ordered by $\mathbb{S}_1$ and not $\mathbb{L}$, indicating that, just as in Fig. 2, the bulk k is determined by $\mathbb{S}_1$. Previous studies of the $\mathbb{L} = \mathbb{S}_1 = 0$ alloy are also plotted.

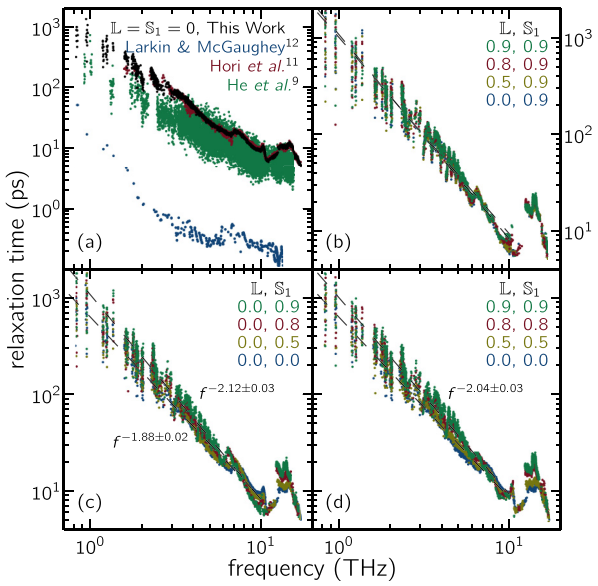

FIG. 4. (Color online) Mode relaxation times for slices through $\mathbb{L}$-$\mathbb{S}_1$ parameter space. (a) Comparison of our fully disordered SiGe structure to previous results. (b) Constant $\mathbb{S}_1$ slice. The majority of modes are unaffected by $\mathbb{L}$. Note the change in ordinate scale. (c) Constant $\mathbb{L}$ slice. All modes are sensitive to $\mathbb{S}_1$. (d) $\mathbb{L} = \mathbb{S}_1$ slice. The relaxation times are nearly identical to those of (c), in agreement with the thermal conductivity trends of Figs. 2 and 3.

with frequencies less than 2 THz carry 88% of the heat in SiGe [14]. Making use of the dispersion calculated for an empirical model of SiGe [11], this translates to a phonon wavelength greater than ∼3.0 nm (longitudinal) or ∼1.8 nm (transverse) in our systems. These wavelengths are greater than the $\mathbb{S}(r)$ decay lengths of about 1.5 nm or less (Fig. 1), which would suggest a reduced dependence of k on $\mathbb{S}_1$ as the system size increases, introducing more long wavelength modes. Yet Fig. 3 shows that the strong dependence of k on $\mathbb{S}_1$ persists out to the bulk limit.

To explore the dependence of k on $\mathbb{S}_1$ further, Fig. 4 shows the normal mode relaxation times. Figure 4(a) compares our results for the completely disordered structure to previous molecular dynamics simulations using normal mode decomposition [9,11,12]. Though each work investigated $Si_{0.5}Ge_{0.5}$ thermal conductivity at 300 K, slightly different simulation and fitting procedures were used. Our relaxation times agree with those of Hori *et al.* [11]. The agreement with He *et al.* [9] is also good, especially considering their use of a Tersoff potential [44] instead of the Stillinger-Weber potential. The relaxation times of Larkin and McGaughey [12] are significantly shorter than the others, although a similar trend is shown. The disagreement may be due to their use of the virtual-crystal modes for the normal mode decomposition [45].

Figures 4(b)–4(d) show the mode relaxation times for two paths between the ordering extrema: ($\mathbb{L}$,$\mathbb{S}_1$) = (0.0,0.0) → (0.9,0.9). That Figs. 4(c) and 4(d) are so similar, and Fig. 4(b) shows no significant change in $\tau(\nu)$ with $\mathbb{L}$, supports the conclusion of Fig. 2: that $\mathbb{S}_1$ accounts for the entire change in k upon ordering.

The relaxation times below 10 THz are roughly fit by a f^{-2} power law [Figs. 4(b)–4(d)]. The fitted exponents fell within -2 ± 0.15 for each plotted ($\mathbb{L}$,$\mathbb{S}_1$) pair. The relaxation times below ∼1.5 THz have a greater variance for two reasons. The total simulation time (4.36 ns) was comparable to the fitted relaxation time, so these modes are nonthermalized, invalidating the assumption of equipartition for those modes. The relaxation times are also comparable to the period of data collection, reducing the accuracy of the Lorentzian fit. It is likely that the power law trend in this regime continues as f^{-2}, but with a reduced variance [2,14], although this cannot be verified by the present simulations.

Figures 4(c) and 4(d) also show a change in the character of the relaxation times, especially in the range of 3–6 THz. The curve is smooth for $\mathbb{S}_1 = 0$. But as $\mathbb{S}_1$ increases, peaks and valleys form where the momentum and energy selection rules for phonon scattering become more and less restrictive. Furthermore, a band gap forms at ∼11 THz.

We therefore attribute the dependence of k on $\mathbb{S}_1$ (instead of $\mathbb{L}$) to the alteration of the phonon eigenvectors caused by short-range ordering. As $\mathbb{S}_1$ increases, the eigenvectors approach those of the zincblende crystal. While high frequency modes might significantly contribute to k in the limit $\mathbb{S}_1 \to 1$, most of the increase for the ordering range studied here is caused by a reduction in the anharmonic scattering of the low frequency modes. The reduction in anharmonic scattering may be due to fewer states that satisfy momentum and energy selection rules, a reduction in the scattering cross section, or both mechanisms. The same trend of k with disorder was observed by Garg *et al.*, who saw a reduction in k with greater disorder when they went from a virtual crystal to an explicitly disordered supercell [14].

They found that the change in k was due to altered mode relaxation times, caused by a modification of the mode eigenvectors.

The findings may be cautiously generalized to other simulated and real alloys provided the thermal conductivities of their disordered states arise primarily from the same mechanisms as those found in the present model of $Si_{0.5}Ge_{0.5}$, namely, the scattering of lattice vibrations by mass disorder. That k depends almost solely on $\mathbb{S}_1$ has implications for the characterization and theoretical modeling of such alloys. When examining an alloy with the purpose of understanding its thermal conductivity or predicting it, a characterization technique sensitive to the short-range order must be used, e.g., diffuse x-ray scattering [46]. Similarly, future efforts to theoretically model thermal transport in ordered alloys should focus on the short-range order or its effect on anharmonic phonon scattering.

In summary, we performed molecular dynamics simulations of a $Si_{0.5}Ge_{0.5}$ alloy, representing a model semiconductor alloy, and calculated the thermal conductivity as it depends on the long- and short-range ordering. We found that the bulk thermal conductivity depends almost wholly on the short-range order of the alloy for a fixed composition. Relaxation time calculations support this dependence. Changes in the character of the mode relaxation times upon ordering imply that the corresponding increase in thermal conductivity is caused by a reduction in disorder-induced anharmonic phonon scattering.

We thank T. Hori, J. Shiomi, Y. He, G. Galli, J. Larkin, and A. McGaughey for sharing their relaxation time data. We are indebted to A. McGaughey and J. Larkin for their comments and insights, and we thank L. Zhigilei for helpful discussion. This work was supported by the National Science Foundation under Grant No. CBET-1134301; and was also conducted with Government support under Contract No. FA9550-11-C-0028 and awarded by the Department of Defense, Air Force Office of Scientific Research, National Defense Science and Engineering Graduate (NDSEG) Fellowship, 32 CFR 168a. C.B. gratefully acknowledges the support and computational resources provided by the NDSEG fellowship and additional support from the Virginia Space Grant Consortium.

[1] B. Abeles, D. S. Beers, G. D. Cody, and J. P. Dismukes, Phys. Rev. **125**, 44 (1962).
[2] B. Abeles, Phys. Rev. **131**, 1906 (1963).
[3] S. T. Huxtable, A. R. Abramson, C.-L. Tien, A. Majumdar, C. LaBounty, X. Fan, G. Zeng, J. E. Bowers, A. Shakouri, and E. T. Croke, Appl. Phys. Lett. **80**, 1737 (2002).
[4] G. Joshi, H. Lee, Y. Lan, X. Wang, G. Zhu, D. Wang, R. W. Gould, D. C. Cuff, M. Y. Tang, M. S. Dresselhaus, G. Chen, and Z. Ren, Nano Lett. **8**, 4670 (2008).
[5] R. Cheaito, J. C. Duda, T. E. Beechem, K. Hattar, J. F. Ihlefeld, D. L. Medlin, M. A. Rodriguez, M. J. Campion, E. S. Piekos, and P. E. Hopkins, Phys. Rev. Lett. **109**, 195901 (2012).
[6] R. B. Wilson and D. G. Cahill, Nat. Commun. **5**, 5075 (2014).
[7] A. Skye and P. K. Schelling, J. Appl. Phys. **103**, 113524 (2008).
[8] J. Chen, G. Zhang, and B. Li, Appl. Phys. Lett. **95**, 073117 (2009).
[9] Y. He, I. Savić, D. Donadio, and G. Galli, Phys. Chem. Chem. Phys. **14**, 16209 (2012).
[10] C. Abs da Cruz, N. A. Katcho, N. Mingo, and R. G. A. Veiga, J. Appl. Phys. **114**, 164310 (2013).
[11] T. Hori, T. Shiga, and J. Shiomi, J. Appl. Phys. **113**, 203514 (2013).
[12] J. M. Larkin and A. J. H. McGaughey, J. Appl. Phys. **114**, 023507 (2013).
[13] A. Kundu, N. Mingo, D. A. Broido, and D. A. Stewart, Phys. Rev. B **84**, 125426 (2011).
[14] J. Garg, N. Bonini, B. Kozinsky, and N. Marzari, Phys. Rev. Lett. **106**, 045901 (2011).
[15] N. Mingo, D. Hauser, N. P. Kobayashi, M. Plissonnier, and A. Shakouri, Nano Lett. **9**, 711 (2009).
[16] Z. Wang and N. Mingo, Appl. Phys. Lett. **97**, 101903 (2010).
[17] A. J. Minnich, M. S. Dresselhaus, Z. F. Ren, and G. Chen, Energy Environ. Sci. **2**, 466 (2009).
[18] C. J. Vineis, A. Shakouri, A. Majumdar, and M. G. Kanatzidis, Adv. Mater. **22**, 3970 (2010).
[19] W. L. Bragg and E. J. Williams, Proc. R. Soc. London, Ser. A **145**, 699 (1934).
[20] J. M. Cowley, Phys. Rev. **77**, 669 (1950).
[21] J. C. Duda, T. S. English, D. A. Jordan, P. M. Norris, and W. A. Soffa, J. Phys.: Condens. Matter **23**, 205401 (2011).
[22] J. C. Duda, T. S. English, D. A. Jordan, P. M. Norris, and W. A. Soffa, J. Heat Transfer **134**, 014501 (2012).
[23] H. Sato, in *Physical Chemistry: An Advanced Treatise*, edited by W. Jost (Academic, New York, 1970), Vol. 10, Chap. 10, p. 579.
[24] The true ordered structure of $Si_{0.5}Ge_{0.5}$ consists of alternating bilayers of Si and Ge in the [111] direction [47]. We took the zincblende structure as the reference since the usage of a single potential for all interactions in the simulation gives all ordered structures equivalent potential energy and many compound semiconductors do order into a zincblende structure, e.g., those of Ref. [48].
[25] P. C. Weakliem and E. A. Carter, Phys. Rev. B **45**, 13458 (1992).
[26] K. L. Whiteaker, I. K. Robinson, J. E. Van Nostrand, and D. G. Cahill, Phys. Rev. B **57**, 12410 (1998).
[27] D. A. McQuarrie, *Statistical Mechanics* (University Science Books, Sausalito, CA, 2000).
[28] A. J. C. Ladd, B. Moran, and W. G. Hoover, Phys. Rev. B **34**, 5058 (1986).
[29] J. Chen, G. Zhang, and B. Li, Phys. Lett. A **374**, 2392 (2010).
[30] In a minority of samples, the noise-to-signal never reached 1000. In these cases, the maximum in the noise-to-signal determined the convergence time.
[31] J. M. Larkin, J. E. Turney, A. D. Massicotte, C. H. Amon, and A. J. H. McGaughey, J. Comput. Theor. Nanosci. **11**, 249 (2014).
[32] J. D. Gale and A. L. Rohl, Mol. Simul. **29**, 291 (2003).
[33] Of course, t_f must be chosen before the maximal τ is known.
[34] M. T. Dove, *Introduction to Lattice Dynamics* (Cambridge University Press, Cambridge, UK, 1993).

[35] Dropping the negative frequency component of $|\dot{Q}(f,\nu)|^2$ causes factors of 2 in Eq. (1) to cancel. The linear, instead of angular, Fourier transform adds a factor of 2π to the expression for τ. See Refs. [31,42].

[36] S. Plimpton, J. Comput. Phys. **117**, 1 (1995), http://lammps.sandia.gov.

[37] F. H. Stillinger and T. A. Weber, Phys. Rev. B **31**, 5262 (1985).

[38] S. Nosé, J. Chem. Phys. **81**, 511 (1984).

[39] W. G. Hoover, Phys. Rev. A **31**, 1695 (1985).

[40] E. S. Landry, Ph.D. thesis, Carnegie Mellon University, 2009.

[41] J. Shiomi, K. Esfarjani, and G. Chen, Phys. Rev. B **84**, 104302 (2011).

[42] A. J. H. McGaughey and J. M. Larkin, Annu. Rev. Heat Transfer **17**, 49 (2014).

[43] J. M. Larkin, Ph.D. thesis, Carnegie Mellon University, 2013.

[44] J. Tersoff, Phys. Rev. B **39**, 5566 (1989).

[45] The disagreement remains perplexing since their calculations of k using the virtual-crystal normal mode relaxation times agree with the k calculated by the Green-Kubo method, as plotted in Fig. 3 and Ref. [43]. Furthermore, the virtual-crystal approximation with *ab initio* force constants produced k values consistent with experiment at 300 K in Ref. [14].

[46] B. E. Warren, *X-Ray Diffraction* (Addison-Wesley, Reading, MA, 1969).

[47] J. Z. Tischler, J. D. Budai, D. E. Jesson, G. Eres, P. Zschack, J.-M. Baribeau, and D. C. Houghton, Phys. Rev. B **51**, 10947 (1995).

[48] I. Vurgaftman, J. R. Meyer, and L. R. Ram-Mohan, J. Appl. Phys. **89**, 5815 (2001).